

# Multi-objective Optimization Design of Adaptive Shading Devices for Office Buildings Considering Daylighting and Visual Comfort

<sup>1</sup>Sayyed Mohammad Mahdi Mirmomtaz, <sup>2\*</sup>Mohammad Baharvand, <sup>3</sup>Narges Dehghan, <sup>4</sup>Tabassom Safikhani

<sup>1</sup> Department of Architecture, Institute of Society and Media, ISF.C., Islamic Azad University, Isfahan, Iran.

<sup>2\*</sup> Department of Architecture, Institute of Society and Media, ISF.C., Islamic Azad University, Isfahan, Iran.

<sup>3</sup> Advancement in Architecture and Urban Planning Research Center, Na.C., Islamic Azad University, Najafabad, Iran.

<sup>4</sup> Tourism, Architecture and Urban Research Center, ISF.C., Islamic Azad University, Isfahan, Iran.

Received 29.01.2025; Accepted 05.10.2025

**ABSTRACT:** Adaptive shading devices offer architects a range of opportunities. These devices not only contribute to unique features and characteristics in building envelopes but, with appropriate design and principled implementation, also enhance visual conditions in interior spaces by providing sufficient levels of daylighting and improving visual comfort. Additionally, they reduce lighting energy consumption in buildings. This study examines four types of adaptive shading systems designed to optimize daylighting and visual comfort. Using a multi-objective optimization approach, various configurations of these systems are examined within the context of a reference office model to achieve a balance between the discussed objectives. For each season, the design alternatives with the highest fitness scores are identified. The findings highlight the relative advantages of horizontal louvers and horizontal sun-breakers over other shading devices. These two adaptive systems provide the reference model with satisfactory daylighting levels (i.e.,  $UDI_{(300-3000lux)} \geq 75\%$ ). Furthermore, regarding glare reduction, full visual comfort is achieved in spring and summer. In fall and winter, when sunlight entering through the southern façade is likely to produce glare, visual comfort is improved by approximately 43% compared to the base case.

**Keywords:** Shading systems, Daylighting, Visual comfort, Adaptive shading device, Multi-objective optimization.

## INTRODUCTION

The concept of dynamism in architecture, particularly in façade design, has gained considerable attention over the past two decades. This concept is most widely implemented through shading systems (e.g., adaptive shading) rather than other primary façade components. Adaptive shading devices, however, are not an entirely new technology in building design. For example, Iranian heritage architecture includes Safavid-era houses equipped with adaptive shading devices that function as dynamic architectural components (Werner, 2013). Historically, these adaptive shading and façade elements were primarily regarded as aesthetic features.

In contrast, today, such systems are valued not only for their aesthetic contribution but also as strategic solutions that provide optimal daylighting within interior spaces. This has positioned them as one of the most rapidly evolving and frequently discussed topics in sustainable architecture. Several studies have demonstrated that the proper and effective design

of such shading systems can optimize daylight levels and visual comfort within a space, while simultaneously reducing energy consumption for lighting. From an architectural perspective, incorporating such dynamic elements in the façade offers an opportunity to explore novel aspects in building envelope design. This approach leads to the creation of an animated façade that, while emphasizing aesthetic aspects, addresses both climatic and functional considerations (Waseef & El-Mowafy, 2017). Consequently, adaptive shading devices are an appealing design choice for designers, architects, and stakeholders alike (Ayyappan & Kumari, 2018). A comparison of fixed and adaptive shading systems indicates the overall superiority of the latter, as fixed devices provide adequate daylighting and efficient glare control only at specific times of the year.

In contrast, adaptive devices, with their capacity to respond to the sun's position and angle, offer more effective glare control,

\*Corresponding Author Email: [Baharvand@iau.ac.ir](mailto:Baharvand@iau.ac.ir)

ORCID: 0000-0003-1638-4910

enhanced visual comfort, and better heat dissipation from solar radiation—qualities particularly beneficial in hot and arid climates. Compared to other building types, office spaces have a heightened need for such adaptive solutions, as they contribute substantially to energy demand in the building sector and require environments that support productivity and well-being. This is because users typically spend extended hours in these spaces with relatively low physical activity. Adaptive shading devices thus offer several key advantages, particularly in terms of visual comfort and glare control, including: increased design flexibility for the building envelope, effective glare control, reduced lighting energy consumption through optimized daylight use, and improved interior environments that support users' productivity and well-being (Bakr, 2019). Consequently, effectively designed adaptive shading devices allow interior spaces to achieve optimal daylight levels while minimizing glare (Mahmoud & Elghazi, 2016).

### Literature Review

Rostamzad et al. examined the performance of an adaptive façade featuring a hexagonal pattern inspired by Slimi motifs. Through shoebox modeling, they evaluated daylight performance using three indices—Spatial Daylight Autonomy (sDA), Annual Sun Exposure (ASE), and Useful Daylight Illuminance (UDI)—and assessed glare control with the Daylight Glare Probability (DGP) index. The study focused on a south-facing office module in Tehran during critical hours of the solstices and equinoxes. Results indicated that with the adaptive façade, UDI increased by 20%, sDA decreased by 3–20%, and ASE was reduced by 40–50% compared to the base case. Additionally, the DGP value remained below 0.35 for most hours, indicating imperceptible glare (Rostamzad et al., 2021).

In a study by Fadaii Ardestani et al., daylight levels and glare control were compared across three classroom configurations within the Faculty of Architecture at Shahid Beheshti University, utilizing both fixed and adaptive shading devices. The findings indicate that the adaptive shading system was more effective in maintaining adequate daylight levels, with classroom daylight varying between -6.55% and +13.09%, compared to the base case. The authors suggest that adaptive shading devices are most effective in spaces with adequate daylight conditions—that is, spaces receiving between 300 and 3000 lux for at least 50% of occupied hours. Furthermore, glare conditions were found to be acceptable in all three configurations with the adaptive shading system, as SVD values remained within the acceptable range (i.e., below 10%) (Fadaii Ardestani et al., 2018).

In their study, Zarkesh et al. employed shoebox modeling to examine the energy, daylight, and glare performance of an adaptive louver system installed on a south-oriented, fully glazed office module in Tehran during the solstice and equinox.

They integrated simulation engines with an optimization engine (i.e., Galapagos) to identify optimal design solutions. Their findings indicate that sufficient daylighting levels (UDI > 50%) are achieved within the spaces, along with effective glare control, which is more accomplished with the adaptive louver system than with a fixed louver system (Zarkesh et al., 2023).

Kheyri and Khalili investigated the performance of an adaptive shading device aimed at enhancing visual comfort in the architectural studios at Tehran University. Daylight performance was assessed from two perspectives: (a) instantaneous performance, measured in lux, and (b) annual performance, evaluated using UDI, sDA, ASE, and average lux. The study was conducted in Tehran during the solstice and equinox, from 8:00 to 18:00, under varying sky conditions—cloudy, semi-cloudy, and cloudless—utilizing Tehran's weather data. According to the research findings, while the adaptive shading device slightly reduced daylight quality, it significantly increased the percentage of time during which daylight levels were adequate (Kheyri & Khalili, 2022).

### MATERIALS AND METHODS

The research workflow comprises three main stages, as illustrated in Fig. 1. In the first stage, a 3D model of the reference office, along with its specifications, is defined using Rhino and Grasshopper. The second stage involves an iterative process wherein Wallacei generates a new design alternative each time by altering the values of design variables. The daylighting and glare performance of this design alternative are then assessed using the Honeybee simulation tool. This process continues until either the specified number of iterations is reached or convergence is achieved. In the final stage, Pareto-optimal solutions are ranked using a fitness function.

### Case Study

The case study is an office space assumed to be located on the middle floor of a multi-story building in Isfahan, with no surrounding natural or constructed obstacles. Given the current trend in office building design in Iran, which favors cellular office spaces, this case study was selected. The dimensions of the model were derived from an assessment of 220 office spaces across nine office buildings in Isfahan, constructed between 2012 and 2022. Table 1 summarizes the findings regarding the ranges of depth and width.

Furthermore, the floor-to-ceiling height in these office spaces ranges from 2.70 meters to 2.80 meters, with the majority measuring 2.80 meters. Based on these findings, the width, depth, and height of the reference office model are set at 6 meters, 6 meters, and 2.8 meters, respectively (Fig. 2).

The typical material used for office buildings in Isfahan typically includes brightly colored walls, a white ceiling, and stone flooring, with respective surface reflectance values of 50%, 70%, and 20%. The window-to-wall ratio (WWR) is

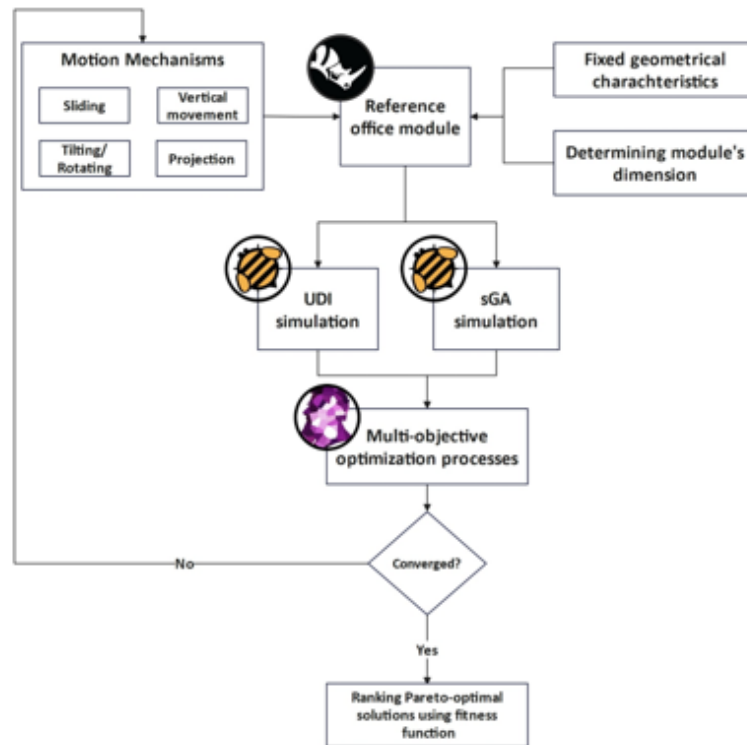


Fig. 1: Research workflow

Table 1: Ranges of Typical Office Space Dimensions Constructed in Isfahan between 2012 and 2022

Orientation	South	
	Depth	Width
Dimension range	3-19 m	3-20 m
Number of types for each dimension	Types 19	Types 14
(Total number of types (southern	Types 72	
Most frequent dimension values	m 6	m 6
Dimensions of the office model in this study	6m*6m	

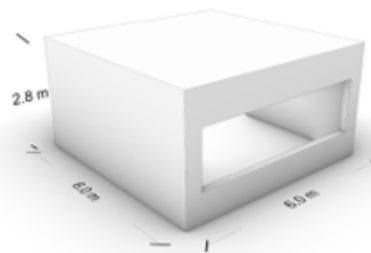


Fig. 2: Dimensions of the reference office model

set at 40%, and the window sill height is 0.8 meters. [Table 2](#) summarizes the design parameters and their respective values.

To incorporate Isfahan's specific environmental parameters, all simulations were conducted using the EnergyPlus Weather (EPW) file IRN\_ES\_Isfahan-Shahid.Beheshti.Intl.AP.408000\_TMYx.2009-2023, sourced from the "Climate.OneBuilding.Org" repository, a standard and widely accepted dataset for building performance simulation. This file provided the necessary hourly inputs to accurately simulate the daylighting behavior and visual comfort outcomes of the south-facing office model.

### Shading Systems

Since this study employs a parametric approach, the shading systems were selected based on the principle that parametric configurations are feasible. Accordingly, the shading systems considered in this study include horizontal louvers (HL), horizontal sun-breakers (HSB), overhangs (OV), and vertical fins (VF) ([Fig. 3](#)).

The motion mechanism of these shading systems involves four types of adjustments in their configuration. Some mechanisms are unique to specific shading systems, while others are common to all shading systems. The first mechanism, common to all systems, is the sliding of slats/fins, achieved through a sliding motion that allows for retraction and extension, resulting in a change in depth ([Fig. 4-a](#)). Another mechanism, exclusive to HL and HSB, involves adjusting the vertical spacing between the fins. This modification alters the shaded area of the glazing, thereby affecting the amount of direct sunlight entering the space ([Fig. 4-b](#)). Moreover, the shading systems can be adjusted by rotating them about their longitudinal axis. For HL and HSB, this axis runs through the center of each slat, while for OV and VF, it corresponds to the axis where the fins are connected to the window system ([Fig. 4-c](#)). Finally, the slats in HL and HSB can be projected outward or retracted, allowing them to adjust their distance from the glazing ([Fig. 4-d](#)).

These motion mechanisms are the design parameters (i.e., genomes) of this study, including tilt angle, distance to the glazing, slat separation, and depth. Various combinations of these parameters yield multiple design alternatives applicable to the southern façade of the reference office module. The ranges and intervals for each parameter are detailed in [Table 3](#).

## Performance Evaluation Metrics

### Daylighting

Through the years, researchers have introduced a variety of metrics to measure daylighting quantity and quality, most notably the useful daylight illuminance (UDI) and the daylight autonomy (DA) family of indices. According to a study by [Kangazian & Emadian Razavi \(2023\)](#), UDI is used in 37% of studies, while the DA family (including DA, cDA, and sDA) is utilized in approximately 30%. Both metrics are dynamic and climate-based, enabling accurate evaluations of buildings' daylighting performance ([Bahdad, Fadzil, Onubi, & BenLasod, 2021; Kangazian & Emadian Razavi, 2023](#)). However, since UDI is a two-tailed metric that measures different thresholds of daylight within a space (e.g., underlit, useful, overlit) ([Carlucci et al., 2015](#)), it will be employed in this study to evaluate the daylighting performance of the shading systems. In this study, UDI calculations will be conducted over one year, considering only the typical working days (i.e., Saturday to Wednesday) and working hours (i.e., 8:00 AM to 5:00 PM) in Iran. The thresholds employed in this research are defined as follows: 0–300 lux for insufficient daylighting, 300–3000 lux for autonomous daylighting, and above 3000 lux for excessive daylighting within the space.

### Glare

Several factors influence users' perception of glare, including the user's position, contrast, vertical illumination, and other related variables. Numerous metrics have been developed to measure glare. Among these, the most comprehensive is the

Table 2: Configuration of the reference office model and the window system

Window system	Sill height		0.8 m
	Window height		1.5 m
	WWR		40%
	Window depth		0.2 m
	Glazing type		Clear air-filled double-glazing
Reference office module	Dimension		
	Orientation		South
	Surface reflectance	Floor	20%
		Walls	50%
		Ceiling	70%

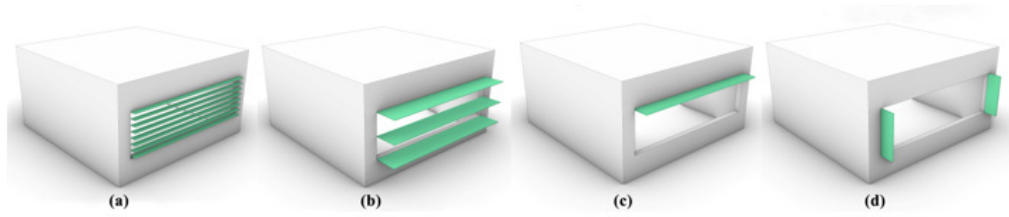


Fig. 3: Considered shading systems include (a) horizontal louver, (b) horizontal sun-breaker, (c) overhang, and (d) vertical fins

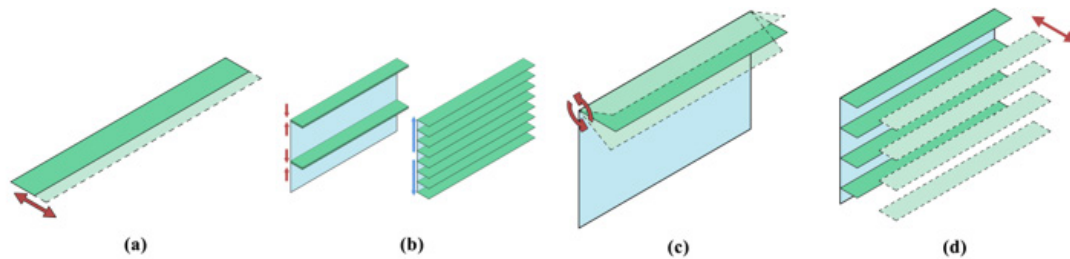


Fig. 4: The motion mechanism of the studied shading systems includes (a) shifting of scale, (b) vertical movement, (c) tilting/rotating, and (d) projection

Table 3: Ranges and increments of design parameters (genomes) for each shading system

Shading System	Horizontal Louver (HL)		Horizontal Sun-breaker (HSB)		(Overhang (OV)		Vertical Fins (VF)	
	Range	Interval	Range	Interval	Range	Interval	Range	Interval
Tilt angle (°)	[-75, +75]	1.00	[-75, +75]	1.00	[0, +75]	1.00	[-75, +75]	1.00
Distance to glazing (m)	[0, 0.3]	0.01	[0, 1]	0.01	-	-	-	-
Slat separation (m)	[0.1, 0.5]	0.01	[0.75, 1.5]	0.01	-	-	-	-
Depth (m)	[0.1, 0.5]	0.01	[0.75, 1.5]	0.01	[0.1, 1]	0.01	[0.1, 1]	0.01

Daylight Glare Probability (DGP), which accounts for key factors responsible for glare (Zomorodian & Tahsildoost, 2017). This metric has been employed in approximately 45% of studies investigating glare (Kangazian & Emadian Razavi, 2023). The DGP quantifies the probability that glare will cause visual disturbances to an individual. However, DGP is an instantaneous-based metric, which makes it challenging to simulate glare conditions over the course of a year (Kangazian & Emadian Razavi, 2023). To address this limitation, Jones (Jones, 2019) introduced the Spatial Glare Autonomy (sGA) metric as a derivative of DGP. sGA quantifies the percentage of views where the DGP remains below 0.4 for at least 95% of the time the space is occupied throughout a year. Generally, a higher sGA value indicates better visual comfort conditions

within a space (Kangazian & Emadian Razavi, 2023).

### Multi-Objective Optimization

Since the 1970s, the multi-objective optimization method has been extensively applied across various fields. Its primary goal is to analyze and address problems involving two or more conflicting objectives, aiming to identify a set of trade-off solutions, often represented as a Pareto front. This is achieved by adjusting decision variables to satisfy given constraints while optimizing the objective functions (Toutou et al., 2018; Wang et al., 2011). Although numerous optimization algorithms have been developed to address multi-objective optimization problems, genetic algorithms (GAs)—a type of evolutionary algorithm inspired by the principles of natural selection—

Table 4: NSGA-II settings

Shading system	Population size	Number of generations	Crossover rate	Mutation rate
Horizontal louver (HL)	20	50	0.9	1/n*
Horizontal sun-breaker (HSB)				
Overhang (OV)	10	25		
Vertical fins (VF)				

\*Wallace automatically calculates the mutation rate according to the number of variables.

\*Wallace automatically calculates the mutation rate according to the number of variables.

have garnered significant attention (Deb, 2011; Kheiri, 2018). Genetic algorithms produce a set of non-dominated solutions, collectively forming the Pareto front, where each solution represents a trade-off among the conflicting objectives (Costa-Carrapiço et al., 2020; Yang, 2014). None of these solutions is inherently superior to another, as improving one objective typically comes at the expense of others (Kangazian, 2022). In this study, the Non-Dominated Sorting Genetic Algorithm II (NSGA-II), a widely recognized method for solving multi-objective optimization problems, is employed. The specific genetic algorithm settings utilized in this research are detailed in Table 4.

#### Ranking Pareto-Optimal Solutions

In contrast to the traditional framework of single-objective problems, where the optimal solution is identified based on a single objective, in cases involving multiple objectives, it is impossible to determine a definitive optimal solution. This is because multiple optimal solutions exist, each considered equally significant (Doumpos et al., 2019; Kangazian, 2022). Therefore, it is necessary to employ multi-criteria decision-making (MCDM) methods to identify an optimal design solution. MCDM methods can simultaneously address conflicting criteria and determine a definitive solution (Kangazian, 2022). Several MCDM methods have been developed to identify the absolute Pareto-optimal (APO) solution. In this study, the fitness of different design alternatives is evaluated using a fitness function developed by Konis et al. (2016). This function can be expressed as Equation 1:

$$Y_i = (UDI_i - UDI_{min}) \left( \frac{100}{UDI_{max} - UDI_{min}} \right) + (sGA_i - sGA_{min}) \left( \frac{100}{sGA_{max} - sGA_{min}} \right)$$

Here,  $Y_i$  Represents the fitness of the considered design alternative,  $i$  denotes its simulation results, min is the minimum value observed among the simulation results for each objective, and max is the maximum value observed. The higher the  $Y_i$  The value of a design alternative is directly related to its fitness compared to others.

## RESULTS AND DISCUSSION

To determine the optimal configuration for each adaptive shading system across different seasons, independent multi-objective optimization processes were conducted on a seasonal basis for each system. Consequently, 16 independent optimization processes were conducted, resulting in 10,000 distinct configurations for the shading systems under consideration. As previously shown in Table 4, for HL and HSB, NSGA-II evaluates 1,000 design alternatives per season, while for OV and VF, it evaluates 250. These solutions represent the most successful trade-offs between the two considered objectives: maximizing visual comfort for users (sGA) and increasing the autonomous daylighting level within the space (UDI300–3000 lux). NSGA-II identified these trade-offs within the solution space of each MOOP. The simulation results for the base model, where no shading device is applied to the southern window of the reference office model, are presented in Table 5. The results show that a minimum acceptable level of daylight (UDI300–3000lux  $\geq$  50%) is achieved during fall and winter, while an adequate level of daylight (UDI300–3000lux  $\geq$  75%) is achieved during spring and summer. However, glare conditions are not within an acceptable range in any season. Specifically, in approximately 25% of the views, DGP exceeded 0.4 for at least 95% of the occupancy period during spring and summer. These issues are even more pronounced during fall and winter, with 57.1% and 56.3% of views exhibiting disturbing or intolerable glare levels (DGP > 0.4).

The APO solutions of each shading system for each season — defined as the five design alternatives with the highest fitness scores — are presented in Tables 6-9.

### Horizontal Louver

The results for HL, shown in Table 6, indicate that these solutions exhibit closely aligned configurations across seasons. However, a noticeable difference in slat separation is observed between spring and the other seasons: in spring, the optimal value for this parameter is 0.39 meters, while in the other seasons, it remains approximately constant at 0.20 meters (Fig. 5-a). Conversely, the optimal slat depth varies depending on the season. In general, the spring solutions exhibit the maximum



Table 5: Daylighting and glare performance of the base case in each season

Season	Performance metrics	
	sGA	UDI-a (%)
Spring	0.761	75.545
Summer	0.773	76.031
Fall	0.571	55.748
Winter	0.563	58.531

slat depth (ranging between 0.4 and 0.47 meters), whereas the summer solutions have the minimum values (0.19 to 0.2 meters) (Fig. 5-b). Furthermore, the optimal tilt angle shows minimal variation across seasons (Fig. 5-c). Additionally, the results suggest that HL should not significantly project toward

or away from the glazing across different seasons. The range of optimal values for the distance-to-glazing parameter is nearly identical in spring and summer and similarly consistent in fall and winter (Fig. 5-d).

Overall, it can be concluded that, when utilizing HL, 'slat

Table 6: Horizontal louver's absolute Pareto-optimal solutions of each season

Season	Solution; Generation	Desing parameters			Results			Ranking*	
		Slat separation (m)	Slat depth (m)	Tilt angle (°)	Distance to glazing (m)	sGA (%)	UDI-a (%)	Fitness score	Rank
Spring	19;13	0.39	0.46	-4	0.12	100	89.73439	2	1
	22;19	0.39	0.47	-4	0.12	100	89.6459	1.986498	2
	15;16	0.38	0.46	-2	0.06	100	89.49347	1.963238	3
	19;12	0.39	0.4	3	0.06	100	89.19015	1.916956	4
	19;15	0.39	0.4	4	0.11	100	89.06306	1.897563	5
Summer	17;20	0.19	0.22	-3	0.11	100	90.23642	2	1
	15;22	0.19	0.22	-2	0.04	100	90.08198	1.952584	2
	22;9	0.19	0.22	-2	0.11	100	90.04953	1.942622	3
	11;5	0.19	0.24	-3	0.09	100	89.86341	1.885481	4
	20;20	0.2	0.2	3	0.05	100	89.76661	1.855762	5
Fall**	21;4	0.21	0.32	0	0.06	100	80.36647	1	1
	21;3	0.21	0.35	0	0.05	100	80.35356	0.959847	2
	22;4	0.21	0.3	3	0.06	100	80.1539	0.3391	3
	16;4	0.19	0.27	4	0.01	100	80.10253	0.179408	4
	12;1	0.19	0.26	5	0.01	100	80.04483	0	5
Winter	16;0	0.16	0.24	1	0.09	100	83.58409	1.992948	1
	19;13	0.18	0.39	-8	0.06	99.3056	83.53521	1.976192	2
	18;2	0.22	0.39	-5	0.01	93.75	83.75209	1.867647	3
	16;1	0.22	0.38	-5	0.01	92.3611	83.661006	1.834411805	4
	20;20	0.21	0.38	-5	0.01	95.1389	82.041185	1.825248128	5

\* The total number of unique Pareto-optimal solutions obtained from the multi-objective optimization process for this shading system, after removing identical and duplicate solutions, is 24 in spring, 28 in summer, 5 in fall, and 41 in winter.

\*\* The number of solutions presented in the table reflects the total number of Pareto-optimal solutions obtained from the multi-objective optimization process.

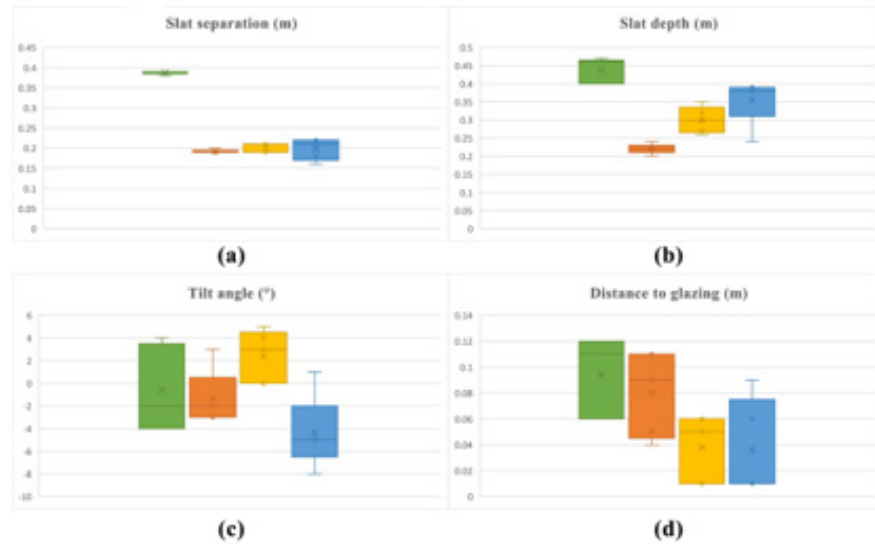


Fig. 5: The range of design parameters (a) slat separation, (b) slat depth, (c) tilt angle and (d) distance to façade when the non-dominated solutions with the highest fitness score of the horizontal louver is applied to the model – Spring is represented by green, summer by orange, fall by yellow, and winter by blue.

separation' and 'slat depth' exert a greater influence on the fitness scores of Pareto-optimal solutions compared to the other two parameters. The seasonal configuration adjustments of HL, based on the APO solution (i.e., Rank 1 fitness score), are presented in Fig. 6.

#### Horizontal Sun-Breakers

The APO solutions for each season when utilizing HSB are presented in Table 7. Evidently, no significant differences in the optimal values obtained for slat separation are observed (Fig. 7-a). Furthermore, the optimal value obtained for slat depth is found to be nearly consistent across the APO solutions of spring and summer. However, spring exhibits a broader range (0.66 m to 0.86 m), while summer presents a narrower range (0.66 m to 0.70 m). Additionally, the results indicate that optimal daylighting and glare conditions within the space

are associated with a gradual increase in slat depth from fall (0.87 m to 0.97 m) to winter (0.96 m to 0.99 m). Notably, the winter range, similar to that for summer, remains relatively narrow (Fig. 7-b). Moreover, the results indicate that the tilt angle range of HSB is similar to that of HL. Comparatively, the tilt angle ranges of HSB's APO solutions for spring and summer are lower than those of fall and winter. This suggests that during spring and summer, direct sunlight can theoretically enter the space more easily, whereas during fall and winter, HSB slightly blocks more direct sunlight from entering the space (Fig. 7-c). Finally, as with HL, the optimal values for distance to the glazing in HSB are slightly higher during spring and summer compared to fall and winter (Fig. 7-d).

Overall, these APO solutions demonstrate that shade depth has a significant influence on the fitness of HSB's design alternatives. The seasonal adjustments in HSB's configuration,

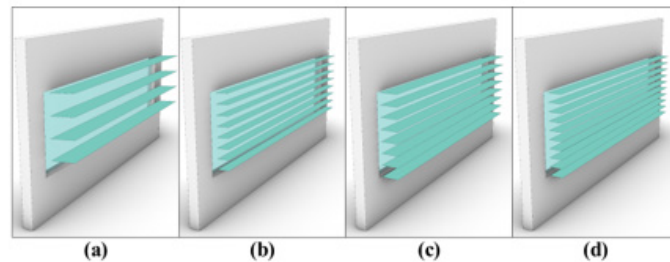


Fig. 6: Configurations of the horizontal louver's most fit non-dominated solution in (a) spring, (b) summer, (c) fall, and (d) winter



Table 7: Horizontal sun-breaker's absolute Pareto-optimal solutions of each season

Season	Solution;Generation	Design parameters				Results		Ranking*	
		Slat separation (m)	Slat depth (m)	Tilt angle (°)	Distance to glazing (m)	sGA (%)	UDI-a (%)	Fitness score	Rank
Spring	25;0	0.58	0.68	-5	0.08	100	90.09821	2	1
	24;10	0.59	0.86	-7	0.09	100	89.9928	1.961302	2
	25;16	0.58	0.83	-6	0.09	100	89.78273	1.884176	3
	23;21	0.57	0.68	-2	0.02	100	89.76661	1.878259	4
	22;20	0.58	0.66	0	0.1	100	89.49347	1.77798	5
Summer	19;0	0.55	0.66	-5	0.07	100	91.02494	2	1
	9;3	0.57	0.68	-5	0.05	100	90.89257	1.955248	2
	20;10	0.53	0.68	-4	0.06	100	90.87605	1.949663	3
	15;23	0.53	0.68	-4	0.09	100	90.71941	1.896709	4
	23;16	0.59	0.7	-3	0.1	100	90.69472	1.888364	5
Fall	47;12	0.57	0.97	1	0.01	98.6111	79.63686	1.678242	1
	35;13	0.56	0.89	3	0.01	99.3056	79.37768	1.485949	2
	31;14	0.56	0.87	4	0.01	100	79.22047	1.408643	3
	49;11	0.61	0.97	2	0.01	97.9166	79.4723	1.392653	4
	31;15	0.55	0.87	1	0.02	96.5278	79.6432	1.385401	5
Winter	47;15	0.55	0.99	-1	0.03	97.9166	83.07718	1.948436	1
	37;17	0.55	0.96	1	0.02	98.6111	82.60367	1.940856	2
	46;1	0.56	0.99	-1	0.03	97.2223	83.09099	1.932205	3
	45;1	0.61	0.99	7	0.02	99.3056	80.80808	1.864787	4
	41;19	0.55	0.96	-2	0.02	94.4444	82.98067	1.858691	5

\* The total number of unique Pareto-optimal solutions obtained from the multi-objective optimization process for this shading system, after removing identical and duplicate solutions, is 40 in spring, 55 in summer, 13 in fall, and 40 in winter.

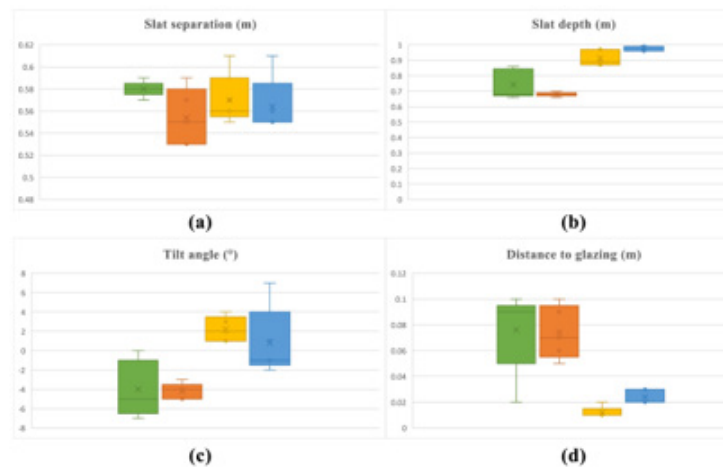


Fig. 7: The range of design parameters (a) slat separation, (b) slat depth, (c) tilt angle and (d) distance to façade when the non-dominated solutions with the highest fitness score of the horizontal sun-breaker is applied to the model – Spring is represented by green, summer by orange, fall by yellow, and winter by blue.

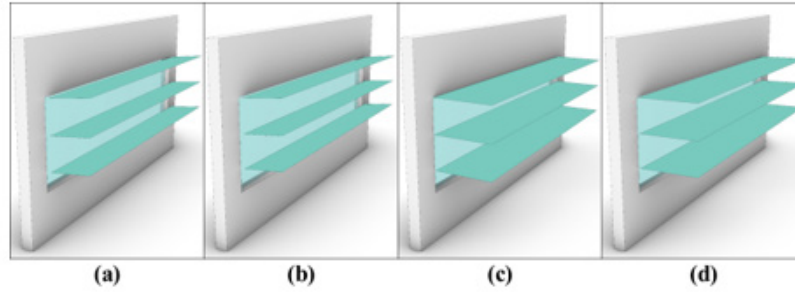


Fig. 8: Configurations of the horizontal sun-breaker's most fit non-dominated solution in (a) spring, (b) summer, (c) fall, and (d) winter

based on the Rank 1 APO solution of each season, are illustrated in Fig. 8.

### Overhang

Table 8 presents OV's APO solutions for each season. As shown, fin depth exhibits minimal variation across seasons,

with all design alternatives achieving near-maximum depth. However, it is noteworthy that the optimal depth decreases slightly in fall (Fig. 9-a). This highlights the negligible impact of fin depth on OV's APO solutions. Furthermore, except for Spring's APO solution at Rank 4, the optimal "tilt angle" remains within a narrow range during spring, summer, and fall. This

Table 8: Overhang's absolute Pareto-optimal solutions of each season

Season	Solution; Generation	Design parameters		Results		Ranking*	
		Fin depth (m)	Tilt angle (°)	sGA (%)	UDI-a (%)	Fitness score	Rank
Spring	21;1	1	50	95.1389	72.72727	1.494835	1
	24;8	0.99	56	95.1389	67.72315	1.241508	2
	23;6	1	51	94.4444	71.98906	1.124114	3
	20;2	1	19	93.0555	82.70615	1	4
	23;2	0.97	62	95.1389	62.95247	1	5
Summer	12;6	1	44	95.8334	76.10929	1.469185	1
	20;6	0.99	47	95.8334	74.3605	1.385071	2
	22;8	1	40	95.1389	77.87556	1.354127	3
	18;7	1	53	96.5278	69.42034	1.34744	4
	11;8	1	54	96.5278	68.75215	1.315301	5
Fall	9;13	0.95	43	84.0278	66.29541	1.343866	1
	23;5	0.97	61	88.1945	58.9727	1.329467	2
	18;7	0.95	51	85.4166	63.52837	1.323571	3
	9;5	0.92	42	83.3333	66.84939	1.314613	4
	16;9	0.97	55	86.1111	61.84292	1.299094	5
Winter	18;8	1	34	81.25	70.4275	1.624479	1
	22;4	1	32	80.5556	70.67637	1.614005	2
	14;1	1	29	79.8611	70.87675	1.6	3
	13;7	0.98	35	81.25	70.03292	1.595789	4
	20;7	0.99	29	78.4722	70.80649	1.537748	5

\* The total number of unique Pareto-optimal solutions obtained from the multi-objective optimization process for this shading system, after removing identical and duplicate solutions, is 16 in spring, 18 in summer, 25 in fall, and 29 in winter.



Fig. 9: The range of design parameters (a) slat depth, and (b) tilt angle when the non-dominated solutions with the highest fitness score of the overhang are applied to the model – Spring is represented by green, summer by orange, fall by yellow, and winter by blue.

consistency contributes to improved control over the amount of direct sunlight entering the space. In contrast, during winter, the tilt angle is reduced, allowing more direct sunlight into the room (Fig. 9-b). It should be noted, however, that an increase in direct sunlight does not necessarily enhance autonomous daylighting levels and may instead lead to excessive levels of daylighting, which, in turn, can cause glare issues.

by green, summer by orange, fall by yellow, and winter by blue.

It can be concluded that OV's APO solutions require minimal seasonal adjustments in the shading configuration. This is illustrated in Fig. 10, which depicts the seasonal variations in OV's configuration, based on the Rank 1 APO solutions for each season.

### Vertical Fins

The APO solutions for VF in each season are outlined in Table 9. Similar to OV, VF's fin depth requires minimal adjustments throughout the year, as it is usually set to the maximum defined depth to prevent direct sunlight as much as possible (Fig. 11-a). Moreover, changes in the tilt angle remain relatively consistent during spring, summer, and fall. However, in winter, there is a wide range of optimal values for this parameter (Fig. 11-b).

Therefore, the APO solutions of VF indicate that minimal changes are required in both design parameters throughout the year. This is illustrated in Fig. 12, which depicts the seasonal variations in VF's configuration, based on the Rank 1 APO solutions for each season.

### Comparative Performance Evaluation

Comparison of the sGA simulation results for the APO solutions of the studied shading systems reveals that HL and HSB demonstrate nearly perfect performance in blocking unwanted daylight, maintaining ideal glare conditions throughout the year. More specifically, as shown in Table 6 and Table 7, when considering all views and 95% of the occupancy period, the DGP values for the APO solutions of HL and HSB remain below 0.4 during spring to fall, and spring and summer, respectively. For the remainder of the year, glare conditions are generally acceptable, with instances of DGP values exceeding 0.4 occurring in a maximum of 7.25% of views, depending on the season and shading system. From a broader perspective, s. 13-a and 13-b illustrate the improvements in glare conditions achieved by applying the APO solutions for each season to the office model. As shown, the sGA values for both HL and HSB during spring and summer increase by approximately

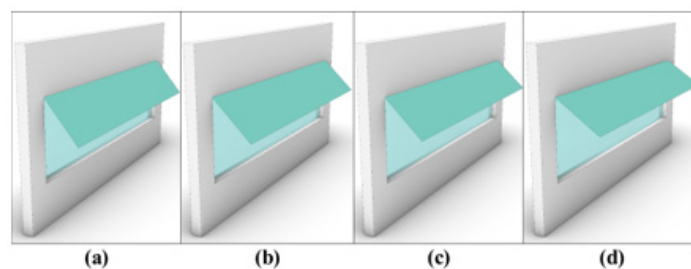


Fig. 10: Configurations of the overhang's most fit non-dominated solution in (a) spring, (b) summer, (c) fall, and (d) winter

Table 9: Vertical Fin's absolute Pareto-optimal solutions of each season

Season	Solution;Generation	Desing param- eters		Results		Ranking*	
		Fin depth (m)	Tilt an- gle (°)	sGA (%)	UDI-a (%)	Fitness score	Rank
<b>Spring**</b>	14;0	1	75	77.0834	77.7968	N/A***	N/A
<b>Summer**</b>	12;1	0.98	71	77.7778	78.16164	2	1
	16;4	0.98	72	77.7778	78.0762	1.390874	2
	17;3	0.97	75	77.7778	78.02138	1	3
	11;1	1	75	77.0834	78.15553	0.956452	4
<b>**Fall</b>	16;1	1	75	53.4722	60.20832	N/A	N/A
<b>Winter</b>	16;0	1	66	52.0833	62.55865	1.747701	1
	19;8	1	75	51.3889	63.0875	1.654051	2
	14;2	1	73	51.3889	62.92078	1.578497	3
	23;9	0.98	-74	52.0833	61.45526	1.247665	4
	19;9	1	62	51.3889	62.09252	1.203142	5

\* The total number of unique Pareto-optimal solutions obtained from the multi-objective optimization process for this shading system, after removing identical and duplicate solutions, is 1 in spring, 4 in summer, 1 in fall, and 19 in winter.

\*\* The number of solutions presented in the table reflects the total number of Pareto-optimal solutions obtained from the multi-objective optimization process.

..Since only one Pareto-optimal solution was obtained for this season, fitness scores cannot be calculated, and ranks cannot be assigned \*\*\*

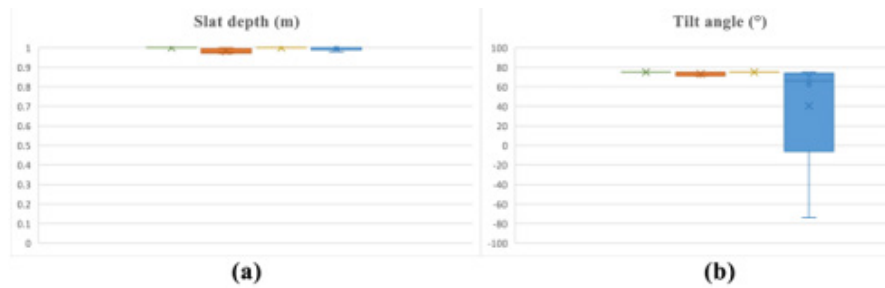


Fig. 11: The range of design parameters (a) slat depth, and (b) tilt angle when the non-dominated solutions with the highest fitness score of the vertical fins are applied to the model – Spring is represented by green, summer by orange, fall by yellow, and winter by blue.

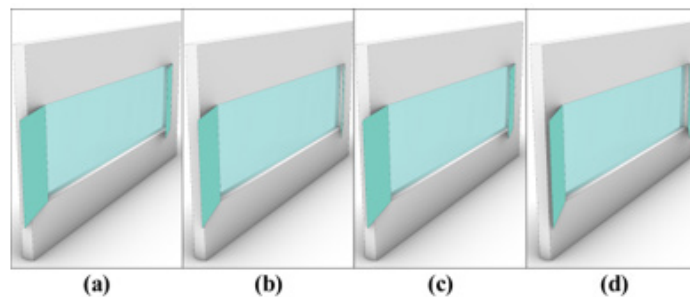


Fig. 12: Configurations of the vertical fins' most fit non-dominated solution in (a) spring, (b) summer, (c) fall, and (d) winter

25% compared to the base case. This is followed by more significant improvements during fall and winter. Notably, except for the HL's APO solutions of fall (all resulting in a 43% improvement), the improvements in glare conditions across other cases vary within a range of 36% to 44%.

Furthermore, for OV's APO solutions, it is evident that during the specified timeframe (i.e., 95% occupancy period) in spring and summer, glare conditions remain at an acceptable level, with sGA values improving by approximately 20% compared to the base case (Fig. 13-c). Additionally, while glare conditions during fall and winter improve by 22% and 31%, respectively, the results in Table 8 indicate that 15% to 20% of views are still subject to disturbing or intolerable glare. Furthermore, VF's APO solutions fail to achieve acceptable glare conditions in any season. During spring and summer, sGA values remain at approximately 77%, while in fall and winter, they range between 51% and 53%. According to Fig. 13-d, utilizing the APO solutions for spring and summer does not significantly improve glare conditions, whereas those for fall and winter result in slightly worse glare conditions compared to the base case, by 3.6% and 4.9%, respectively.

Regarding autonomous useful daylight illumination (UDI300-300lux) results, the findings indicate that the performances of HL and HSB are comparable. During the spring and summer, daylighting alone is sufficient to illuminate the task area for approximately 90% of the occupancy period, with electric lighting required for only about 10% of the time (Tables 6 and 7). In fall and winter, despite a relative reduction in

autonomous daylighting levels, adequate daylighting levels are still achieved during approximately 80% and 83% of the occupancy periods, respectively. A comparison with the base model shows that applying HL's and HSB's APO solutions to the office results in approximately a 15% improvement in spring and summer, and a 25% improvement in fall and winter (Fig.13a and Fig.13b). Furthermore, among OV's APO solutions, excluding those of winter, which consistently achieve a UDI value of approximately 70%, the daylighting performance of the APO solutions of other seasons varies considerably. This contrasts with other shading systems, where the Rank 1 to Rank 5 APO solutions of each season exhibit comparable performance. Consequently, as shown in Fig. 13-c, the daylighting performance of OV's APO solutions of different seasons varies significantly, ranging from -13% to +12% compared to the base case.

Furthermore, similar to HL and HSB, VF's APO solutions of spring and summer provide a higher level of autonomous daylighting compared to those of fall and winter. However, unlike HL's and HSB's APO solutions, which provide adequate levels of autonomous daylighting throughout the year, those of VF achieve such levels only during spring and summer. However, VF's APO solutions of fall and winter do not perform poorly in this regard, as an acceptable level of autonomous daylighting is still achieved during these seasons. Nevertheless, as shown in Fig. 13-d, none of VF's APO solutions contributes to a significant improvement in daylighting levels compared to the base model, with UDI values improving by approximately

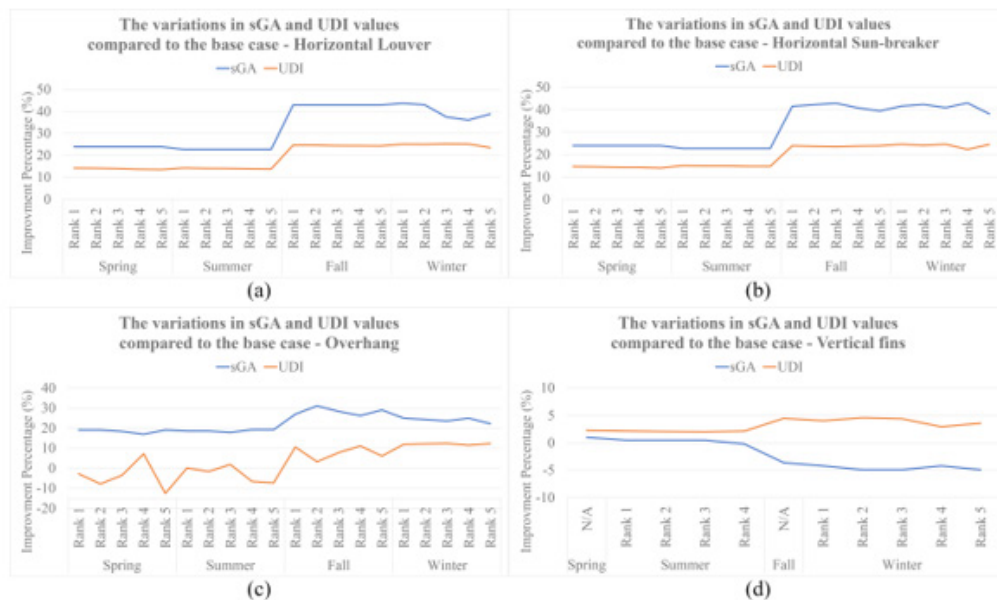


Fig. 13: The variations in sGA (blue) and UDI (orange) values in the non-dominated solutions with the highest fitness score of (a) horizontal louver, (b) horizontal sun-breaker, (c) overhang, and (d) vertical fins compared to the base case

2% in spring and summer, 3% in fall, and 4.5% in winter.

## CONCLUSION

This research investigated the performance of four types of adaptive shading devices, aiming to maximize autonomous daylighting and minimize glare. The shading system configurations were adjusted at quarterly intervals (i.e., seasonally). Different configurations for each shading system were evaluated in each season using separate multi-objective optimization processes. Pareto-optimal solutions were determined, and the absolute Pareto-optimal solutions were identified using a fitness function. This process revealed that the primary design parameters for identifying the absolute Pareto-optimal solutions for each season are slat separation and slat depth for HL, slat depth for HSB, tilt angle for OV, and tilt angle and fin depth for VF. In general, the absolute Pareto-optimal solutions maximize autonomous daylight during spring and summer; however, they provide lower daylight levels in the fall, with a slight increase observed in the winter. Specifically, HL and HSB's absolute Pareto-optimal solutions demonstrate comparable daylighting performance throughout the year, maintaining an adequate daylighting level ( $UDI_{300-3000lux} \geq 75\%$ ). Their glare performance is also comparable: during spring and summer, they provide a virtually glare-free environment. During fall and winter, when the probability of glare increases in southern-facing buildings, these design alternatives improve glare conditions by approximately 43% compared to the base case. In contrast, when applying OV's absolute Pareto-optimal solutions to the office, glare conditions for users during fall and winter are compromised, with 15% to 20% of views experiencing disturbing or intolerable glare. Their daylighting performance also varies significantly, with UDI values ranging from -13% to +12% compared to the base model, achieving only a minimally acceptable daylighting level ( $UDI \geq 3000lux > 50\%$ ). Furthermore, VF's absolute Pareto-optimal solutions have either a neutral or adverse impact on glare conditions. During spring and summer, glare shows no significant improvement compared to the base case. In contrast, in fall and winter, sGA values decrease by 3.6% and 4.9%, respectively, resulting in undesirable glare conditions throughout the year. These design alternatives also provide negligible improvements to autonomous daylighting levels, with UDI values increasing by approximately 2% in spring and summer, and by 3% and 4.5% in fall and winter, respectively.

While this study focuses on performance-based optimization of adaptive shading systems, it is important to consider their real-world feasibility. Many of the optimal configurations identified, particularly for HL and HSB, are within the geometrical and mechanical limits of commercially available dynamic façade systems. However, practical implementation may be constrained by factors such as initial investment costs, structural integration requirements, control system complexity,

and long-term maintenance demands. For example, fine-tuning slat spacing or projection depth seasonally may require advanced control algorithms and responsive actuators, which could pose operational challenges. Future research should evaluate these optimal designs through cost-benefit and lifecycle assessments to determine their viability in actual office building retrofits or new construction projects.

From a practical standpoint, the study's findings suggest several recommendations for designers and decision-makers. In hot, arid climates with strong southern exposure, horizontal louvers and horizontal sun-breakers offer the most reliable year-round performance in terms of both glare mitigation and daylight availability. To maximize their benefits, these systems should be integrated with intelligent lighting control systems that respond to dynamic daylighting conditions. Although the optimization framework presented in this research can be adapted to other building types, such as classrooms or public facilities, certain elements of the simulation process are context-specific. Parameters such as space function, occupancy profiles, and geometric dimensions were calibrated for office use and may require significant adjustment when applied to different building typologies. Therefore, while the general methodology remains applicable, its transfer to other contexts should be approached with careful adaptation and consideration.

## AUTHOR CONTRIBUTIONS

S.M.M. Mirmomtaz: Literature review, conceptualization, data curation, model training, validation, preparation of main manuscript, and editing. M. Baharvand, N. Dehghan, and T. Safikhani: Supervision, Project administration, Formal analysis.

## CONFLICT OF INTEREST

The authors declare no potential conflict of interest regarding the publication of this work. In addition, the authors have acknowledged the ethical issues, including plagiarism, informed consent, misconduct, data fabrication and/or falsification, double publication and/or submission, and redundancy.

## REFERENCES

- Ayoub, M. (2019). 100 Years of Daylighting: A chronological Review of Daylight Prediction and Calculation Methods. *Solar Energy*, 194, 360-390. <https://doi.org/10.1016/j.solener.2019.10.072>
- Ayyappan, K. L., & Kumari, R. M. (2018). A Review on the Application of Kinetic Architecture in Building Façades. *Journal of International Research Journal of Engineering and Technology (IRJET)*, 5:1726-1743. <https://www.irjet.net/archives/V5/i8/IRJET-V5I8298.pdf>
- Bahdad, A. A. S., Fadzil, S. F. S., Onubi, H. O., & BenLasod, S. A. (2021). Sensitivity Analysis Linked to Multi-objective Optimization for Adjustments of Light-Shelves Design



Parameters in Response to Visual Comfort and Thermal Energy Performance. *Journal of Building Engineering*, 44, 102996. <https://doi.org/10.1016/j.jobbe.2021.102996>

Bakr, A. O. (2019). Kinetic Façades: the New Paradigm Shift in Architecture Toward an Environmental Design Performance. *Journal of Arts, Literature, Humanities and Social Sciences*, 43, 577-590. <https://doi.org/10.33193/JALHSS.43.29>

Carlucci, S., Causone, F., De Rosa, F., & Pagliano, L. (2015). A Review of Indices for Assessing Visual Comfort with a View to Their Use in Optimization Processes to Support Building Integrated Design. *Renewable and Sustainable Energy Reviews*, 47, 1016-1033. <https://doi.org/10.1016/j.rser.2015.03.062>

Costa-Carrapiço, I., Raslan, R., & González, J. N. (2020). A Systematic Review of Genetic Algorithm-based Multi-objective Optimisation for Building Retrofitting Strategies Towards Energy Efficiency. *Energy and Buildings*, 210. <https://doi.org/10.1016/j.enbuild.2019.109690>

Deb, K. (2011). Multi-objective Optimisation Using Evolutionary Algorithms: An Introduction. In L. Wang, A. H. C. Ng, & K. Deb (Eds.), *Multi-objective Evolutionary Optimisation for Product Design and Manufacturing* (pp. 3-34). London: Springer London. [https://doi.org/10.1007/978-3-030-11482-4\\_1](https://doi.org/10.1007/978-3-030-11482-4_1)

Doumpos, M., Figueira, J. R., Greco, S., & Zopounidis, C. (2019). *New Perspectives in Multiple Criteria Decision Making: Innovative Applications and Case Studies*. Springer International Publishing. <https://link.springer.com/book/10.1007/978-3-030-11482-4>

Fadaii Ardestani, M. A., Nasserli Mobaaraki, H., Ayatollahi, M. R., & Zomorrodian, Z. S. (2019). The Assessment of Daylight and Glare in Classrooms Using Dynamic Indicators: The Case of SBU Faculty of Architecture and Urban Planning. *Soffeh*, 28(83), 25-40. [In Persian]. Retrieved October 15, 2024, from [https://soffeh.sbu.ac.ir/article\\_100759.html](https://soffeh.sbu.ac.ir/article_100759.html)

Jones, N. L. (2019). Fast Climate-based Glare Analysis and Spatial Mapping. In *Proceedings of Building Simulation 2019: 16th Conference of IBPSA*. Rome, Italy: IBPSA. Retrieved November 19, 2024, from <https://www.researchgate.net/publication/335473181>

Kangazian, A. (2022). *Designing an Office Building in Isfahan City with Simultaneous Optimization of Energy Consumption and Visual Comfort Approach (Via Parametric Simulation of Daylight Control Systems)* [Master's thesis, Yazd University]. [In Persian]. Retrieved November 8, 2024, from <https://ganj.irandoc.ac.ir/#/articles/1db8a93d69516a8ff297f7bc2df49563>

Kangazian, A., & Emadian Razavi, S. Z. (2023). Multi-criteria Evaluation of Daylight Control Systems of Office Buildings Considering Daylighting, Glare, and Energy Consumption. *Solar Energy*, 263, 111928. <https://doi.org/10.1016/j.solener.2023.111928>

Kheiri, F. (2018). A Review on Optimization Methods Applied in Energy-efficient Building Geometry and Envelope Design.

*Renewable and Sustainable Energy Reviews*, 92, 897-920. <https://doi.org/10.1016/j.rser.2018.04.080>

Kheyri, N., & Khalili, A. (2022). Daylight Quality Evaluation of Pardis Architecture Atelier Building, Faculty of Fine Arts, Tehran. *Journal of Life Space*, 1(2), 41-58. [In Persian]. Retrieved October 29, 2024, from <https://sanad.iau.ir/Journal/ljsj/Article/951822>

Konis, K., Gamas, A., & Kensek, K. (2016). Passive Performance and Building Form: An Optimization Framework for Early-stage Design Support. *Solar Energy*, 125, 161-179. <https://doi.org/10.1016/j.solener.2015.12.020>

Mahmoud, A. H. A., & Elghazi, Y. (2016). Parametric-based Designs for Kinetic Façades to Optimize Daylight Performance: Comparing Rotation and Translation Kinetic Motion for Hexagonal Façade Patterns. *Solar Energy*, 126, 111-127. <https://doi.org/10.1016/j.solener.2015.12.039>

Rostamzad, S., Feizi, M., Sanaieian, H., & Khakzand, M. (2021). Parametric Design of a Kinetic Façade for the Improvement of Daylight Performance and Visual Comfort: Case Study of an Office Space in Tehran. *Journal of Architecture and Urban Planning*, 13(31), 85-100. [In Persian]. <https://doi.org/10.30480/aup.2020.2421.1464>

Toutou, A., Fikry, M., & Mohamed, W. (2018). The Parametric-Based Optimization Framework: Daylighting and Energy Performance in Residential Buildings in Hot Arid Zone. *Alexandria Engineering Journal*, 57(4), 3595-3608. <https://doi.org/10.1016/j.aej.2018.04.006>

Wang, L., Ng, A. H. C., & Deb, K. (Eds.). (2011). *Multi-objective Evolutionary Optimisation for Product Design and Manufacturing* (1st ed.). Springer. <https://doi.org/10.1007/978-0-85729-652-8>

Waseef, A. A., & El-Mowafy, B. N. (2017). Towards a New Classification for Responsive Kinetic Façades. In *Proceedings of the Memaryat International Conference (MIC)*, Jeddah, Saudi Arabia. Retrieved November 26, 2024, from [https://www.academia.edu/download/87699055/TOWARDS\\_A\\_NEW\\_CLASSIFICATION\\_FOR\\_RESPONSIVE\\_KINETIC\\_FACADES.pdf](https://www.academia.edu/download/87699055/TOWARDS_A_NEW_CLASSIFICATION_FOR_RESPONSIVE_KINETIC_FACADES.pdf)

Werner, C. D. M. (2013). *Transformable and Transportable Architecture: Analysis of Buildings Components and Strategies for Project Design* [Master's thesis, Universitat Politècnica de Catalunya]. Retrieved October 7, 2024, from <https://upcommons.upc.edu/bitstreams/d5b68f1f-ebad-4e2f-a8f3-4f3a0823202c/download>

Yang, X.-S. (2014). Multi-objective Optimization. In X.-S. Yang (Ed.), *Nature-inspired Optimization Algorithms* (pp. 197-211). Elsevier. [https://www.researchgate.net/publication/263171713\\_Nature-Inspired\\_Optimization\\_Algorithms](https://www.researchgate.net/publication/263171713_Nature-Inspired_Optimization_Algorithms)

Zarkesh, A., Shahmoradi, M., & Yeganeh, M. (2023). Energy Consumption Optimization and Visual Comfort in Office Space Using Dynamic Shading Devices. *Journal of Sustainable*

Architecture and Urban Design, 11(1), 1–28. [In Persian].  
<https://doi.org/10.22061/jsaud.2023.9240.2078>  
Zomorodian, Z. S., & Tahsildoost, M. (2017). Assessment of

Window Performance in Classrooms by Long-term Spatial  
Comfort Metrics. Energy and Buildings, 134, 80–93. <https://doi.org/10.1016/j.enbuild.2016.10.018>



© 2025 by author(s); Published by Science and Research Branch Islamic Azad University, This work for open access publication is under the Creative Commons Attribution International License (CC BY 4.0). (<http://creativecommons.org/licenses/by/4.0/>)